Tetrahedron 64 (2008) 8464–8475

Contents lists available at ScienceDirect

Tetrahedron

journal homepage: www.elsevier.com/locate/tet

Integrating replication processes with mechanically interlocked molecular architectures

Annick Vidonne, Douglas Philp *

EaStCHEM and Centre for Biomolecular Sciences, School of Chemistry, University of St. Andrews, North Haugh, St. Andrews, Fife KY16 9ST, UK

ARTICLE INFO

Article history:
Received 28 March 2008
Received in revised form 6 May 2008
Accepted 9 May 2008
Available online 14 May 2008

Keywords:
Molecular recognition
Self-replication
Rotaxanes
Kinetics

ABSTRACT

A kinetic model for the integration of self-replication with the formation of a mechanically interlocked molecular architecture, namely a rotaxane, is presented. The logical steps required to convert this model into molecular structures through consideration of the design criteria highlighted by the model are discussed and executed. Ultimately, despite careful design, the rotaxane synthesised did not replicate as expected. The reasons for this failure are traced by experiment and computation to the sub-optimal association constant for the pseudorotaxane complex required to form the replicating rotaxane. Additionally, a deleterious supramolecular steric effect, operating through the proximity of the macrocyclic component of the pseudorotaxane to the transition state for the stoppering reaction is identified computationally.

1. Introduction

Recent advances in supramolecular synthesis have permitted the fabrication[1] of discrete, structurally intricate nanometre-scale objects,[2] molecular machinery[3] and periodic structures.[4] Sophisticated supramolecular hierarchies[5] of this sort can be constructed through the precise arrangement of structural subunits through algorithmic self-organisation and self-assembly. Thus, the construction of structurally diverse families of novel, intelligent materials—possessing programmability, addressability and desirable physical[6] attributes—has become feasible. Although approaches based on self-assembly are versatile, the production of the basic subunits for any assembly process currently relies upon traditional synthetic methodologies. Drexler[7] highlighted a radical alternative—the fabrication of replicateable networks via atom-by-atom engineering. However, this proposal has been described[8] as implausible and unrealistic. Despite this criticism, an attractive alternative to traditional synthetic approaches is a strategy based on replication processes. In this approach, the building blocks for the subsequent self-assembly processes are themselves capable of their own synthesis through recognition-mediated processes.

In the last 15 years, several examples[9] of self-replicating systems capable of templating and catalysing their own synthesis have appeared[10] in the chemical literature. Almost all of the examples of synthetic self-replicators reported in this period have been based on the kinetic model[11] shown in Figure 1.

This minimal model of self-replication contains three distinct reaction channels. The first is the uncatalysed bimolecular reaction between reagents **A** and **B** to afford the template **T**. A key requirement of the model is that **A** and **B** bear complementary recognition sites. One consequence of the presence of these recognition sites is that **A** and **B** can associate with each other to

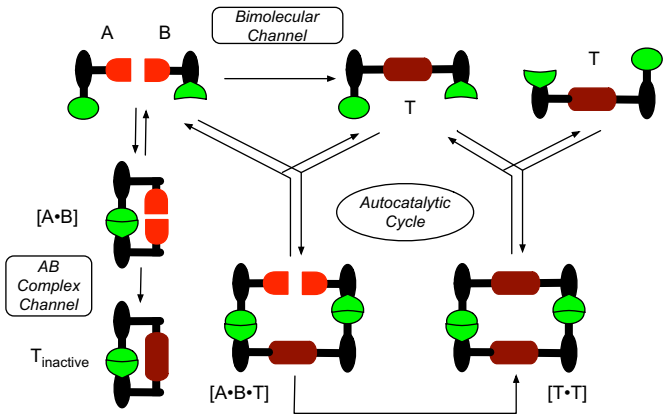

Figure 1. The minimal model of self-replication. Reagents **A** and **B** can react through three pathways—an uncatalysed bimolecular reaction, a recognition-mediated pseudounimolecular pathway mediated by a binary complex [**A**·**B**] and a recognition-mediated pseudounimolecular autocatalytic cycle mediated by a ternary complex [**A**·**B**·**T**].

* Corresponding author.
E-mail address: dp12@st-andrews.ac.uk (D. Philp).

0040-4020/$ – see front matter © 2008 Elsevier Ltd. All rights reserved.
doi:10.1016/j.tet.2008.05.049

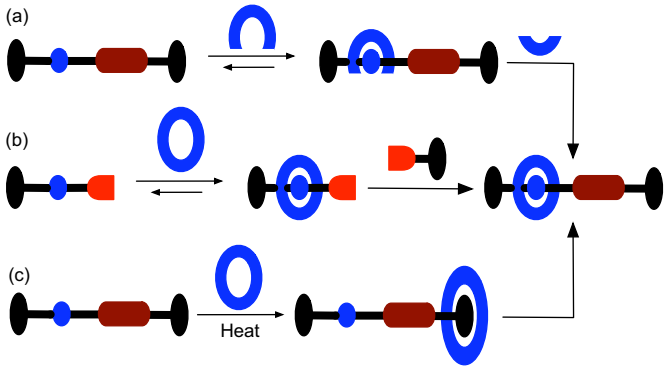

Figure 2. Methods of rotaxane formation. (a) Clipping: a recognition site within the thread-like component is used to template the formation of the macrocyclic component of the rotaxane. (b) Threading and stoppering: a pseudorotaxane complex between a linear molecule and a macrocycle is captured by covalent bond formation between a stoppering reagent and the pseudorotaxane complex. (c) Slippage: the two pre-formed components of the rotaxane can associate through a temporary increase in the mean free path available through the macrocycle cavity, usually accomplished by heating.

form a binary complex, [**A**·**B**]. The formation of this complex opens a second reaction channel—the binary or [**A**·**B**] complex channel—in which **A** and **B** are preorganized[12] with respect to each other and the reaction between them is pseudointramolecular. The product of this reaction channel forms a closed template $\mathbf{T}_{\mathbf{inactive}}$, in which the recognition used to assemble the binary complex lives on in the template, thus, although rate acceleration is achieved by this mechanism, this template is catalytically inert. The third reaction channel available to the system is the autocatalytic[13] cycle. In this channel, **A** and **B** bind reversibly to the open template **T** to form a catalytic ternary complex [**A**·**B**·**T**]. In a manner similar to the [**A**·**B**] complex, the reaction between **A** and **B** is also rendered pseudointramolecular. Bond formation occurs between **A** and **B** to give the product duplex [**T**·**T**], which then dissociates to return two molecules of **T** to the start of the autocatalytic cycle. Thus, assuming that the open template **T** presents its recognition sites in the correct orientation, it can act as a template for its own formation, transmitting molecular information through the formation of identical copies of itself.

Our initial forays[14] in the field of molecular self-replication focused on the utilisation of bifunctional precursor subunits that incorporate mutually complementary recognition elements (essential for reversible, intermolecular assembly) and reactive functionalities (essential for the irreversible construction of scaffolds). These features are combined to engineer linear self-complementary platforms capable of autocatalytic self-propagation through the mechanism illustrated in Figure 1. The rapid developments in the synthesis and exploitation of mechanically interlocked molecules[15] in chemistry, such as catenanes and rotaxanes, have been

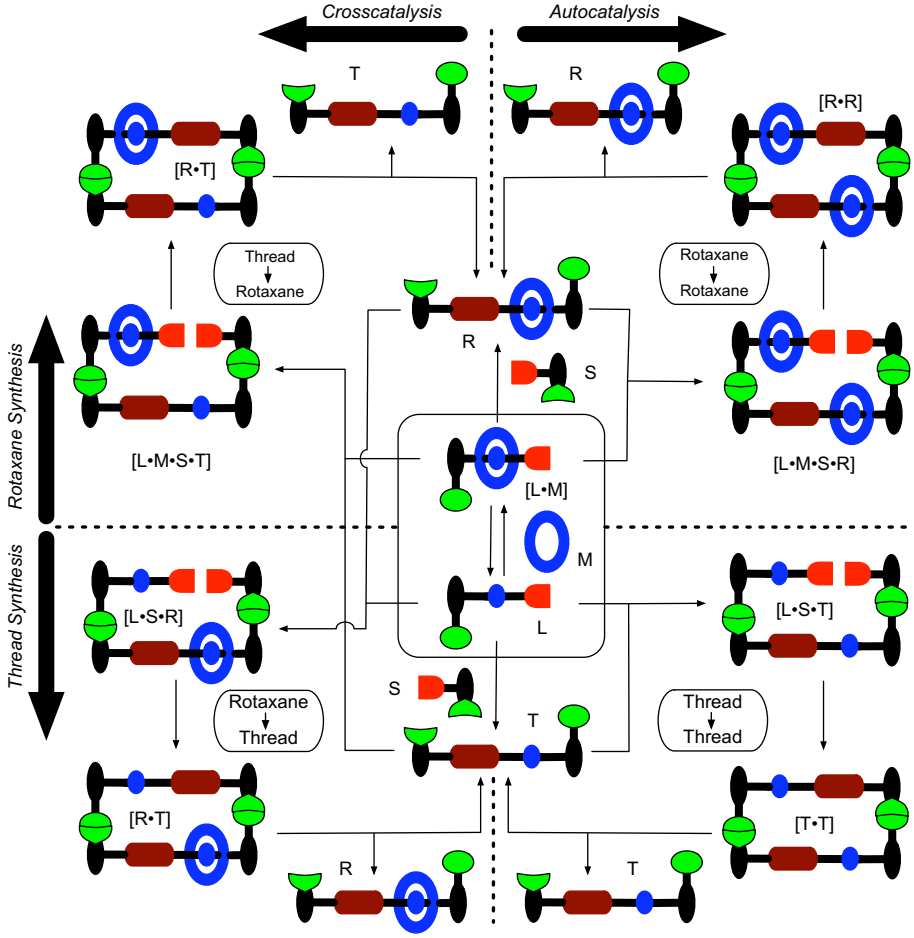

Figure 3. The minimal kinetic model for a replicating rotaxane based on the threading and stoppering approach. Four interlinked catalytic cycles operate emanating from the central binding event (boxed), the reversible formation of the [**L**·**M**] pseudorotaxane complex. Above the dotted horizontal line, rotaxane synthesis is accomplished through either crosscatalysis (top left) by thread **T** or autocatalysis (top right) by rotaxane **R**. Below the dotted horizontal line, thread synthesis is accomplished through either crosscatalysis (bottom left) by rotaxane **R** or autocatalysis (bottom right) by thread **T**. It is assumed that reactions through binary complexes can be removed by careful design and are not shown for clarity.

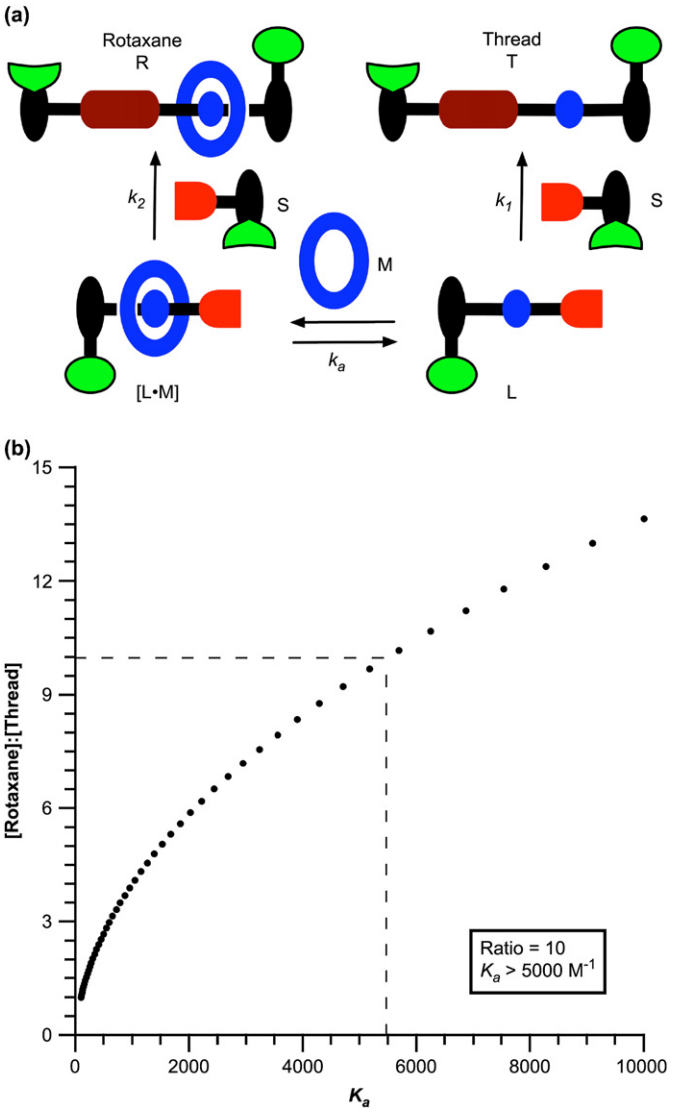

Figure 4. (a) Simple kinetic model for rotaxane formation. Stoppering reagent **S** can react with either unbound linear component **L** (k_1) or the complex between **L** and macrocycle **M** (k_2). The [**L**·**M**] complex has a stability defined by K_a. (b) Ratio of rotaxane **R**/thread **T** as a function of K_a assuming $k_1=k_2=1.67\times10^{-3}$ M^{-1} s^{-1}.

contemporaneous with the emergence of synthetic replicating systems. This upsurge in interest[16] in mechanically interlocked molecules has been made possible by the exploitation of recognition-mediated processes for their synthesis. However, despite the obvious advantages, the combination of the recognition-mediated synthesis of a mechanically linked architecture and the amplification of this structure by replication—similar in spirit to the replicatable networks described by Drexler—has remained an unexplored area. Here, we report our first attempts at integrating the synthesis of a [2]rotaxane within a self-replicating framework.

2. Results and discussion

Conceptually, the integration of the synthesis of a [2]rotaxane within a self-replicating system requires a number of design choices to be made. Firstly, the method of rotaxane synthesis (Fig. 2) must be chosen.

Consideration of how the processes highlighted in Figures 1 and 2 might be integrated leads rapidly to the realisation that the threading and stoppering approach to rotaxane synthesis (Fig. 2b) is the only one that can be combined with the synthesis of a linear template through replication. Replication requires the formation of covalent bond at some point along the length of a rigid, linear molecule. Of the three possible modes of rotaxane synthesis available, only threading and stoppering has the same requirement for covalent bond formation. In the other two cases, the linear component is already intact at the time of rotaxane formation. Recognising this requirement allows us to envisage the expanded replication scheme depicted in Figure 3. The template **T** (which forms the thread-like component of the rotaxane) has been extended compared to the template **T** shown in Figure 1, and now incorporates an additional binding site (blue in Fig. 3).

The introduction of this additional binding site opens up a much more complex network of catalytic pathways. This kinetic scheme for the formation of replicating rotaxane actually contains four interlinked catalytic cycles—the autocatalytic cycle in the lower right of the kinetic scheme corresponds to the autocatalytic cycle present in Figure 1. All of these four cycles emanate from the central binding event (Fig. 3), the reversible formation of the [**L**·**M**] complex, with pseudorotaxane geometry, through the association of macrocycle **M** with the linear component **L**. Above the dotted horizontal line, the [**L**·**M**] complex can react with the stoppering reagent **S** to form rotaxane **R** (this process is analogous to the bimolecular channel in Fig. 1). Rotaxane **R** can then enter an autocatalytic cycle (top right, Fig. 3)—collecting the [**L**·**M**] complex and stoppering reagent **S** and catalysing the formation of a second molecule of rotaxane **R**. Alternatively, rotaxane **R** can enter a crosscatalytic cycle (lower left, Fig. 3)—collecting the unbound linear component **L** and stoppering reagent **S** and catalysing the formation of a molecule of thread **T**. Conversely, below the dotted horizontal line, unbound linear component **L** can react with the stoppering reagent **S** to form thread **T** (once again, this process is analogous to the bimolecular channel in Fig. 1). Thread **T** can then enter a crosscatalytic cycle (top left, Fig. 3)—collecting the [**L**·**M**] complex and stoppering reagent **S** and catalysing the formation of a molecule of rotaxane **R**. Alternatively, thread **T** can enter an autocatalytic cycle (lower right, Fig. 3)—collecting the unbound linear component **L** and stoppering reagent **S** and catalysing the formation of a second molecule of thread **T**.

It is clear from this analysis that the position of the equilibrium between the linear component **L** and macrocycle **M** and the corresponding [**L**·**M**] complex is central to the success of this enterprise. Replication processes operate best at low concentrations—where the relative importance of the bimolecular reaction channel, in a kinetic sense, is minimised. This objective clearly requires the association constant K_a for the [**L**·**M**] complex to be high. Typically, our successful replicating systems[17] operate in a concentration range from 10 to 25 mM. Using this knowledge, we can assess the required target K_a for the additional binding site that will be used in the **L** component (Fig. 3) to associate macrocycle **M**.

In order to make this assessment, we employed (Fig. 4a) a simple kinetic scheme in which rotaxane synthesis is viewed as two parallel kinetic pathways operating either side of an equilibrium. Assuming that **L** and [**L**·**M**] have the same reactivity, we can assess the ratio of rotaxane to thread component in the reaction mixture across a range of K_a values for the [**L**·**M**] complex through kinetic simulation. Taking $k_1=k_2=1.67\times10^{-3}$ M^{-1} s^{-1} and initial concentrations of **L**, **S** and **M** of 20 mM, Figure 4b illustrates how the [rotaxane]/[thread] composition in the reaction mixture after 8 h varies with K_a. We would view an acceptable level of selectivity for rotaxane as being at least 10:1, therefore we had to target a K_a for the [**L**·**M**] complex of >5000 M^{-1}. Accordingly, we identified pyridone as potential binding site, and designed and synthesised (see Supplementary data) macrocycle **1** as a host to complex guests (Fig. 5) incorporating this recognition motif. During the course of this work, Chiu and co-workers independently reported[18] the

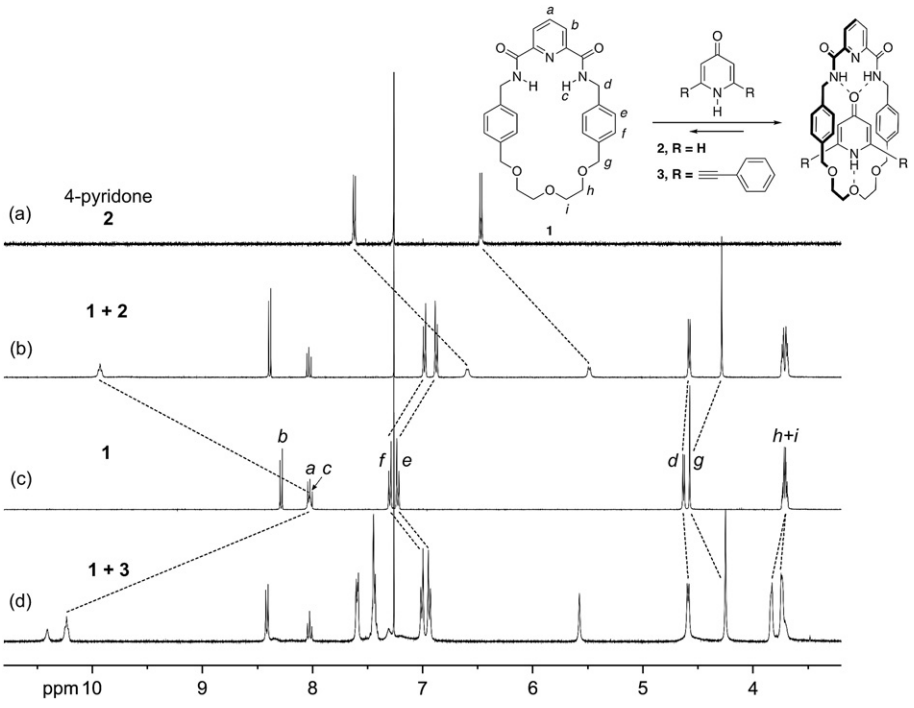

Figure 5. Partial ^{1}H NMR spectra (400.1 MHz, 25 °C, $CDCl_3$, 25 mM) of (a) 4-pyridone **2**, (b) an equimolar mixture of macrocycle **1** and 4-pyridone **2**, (c) macrocycle **1** and (d) an equimolar mixture of macrocycle **1** and extended pyridone **3**. Dashed lines are shown to connect resonances for specific protons in the bound and unbound states. The ^{1}H NMR spectrum of **3** is not shown as a result of the limited solubility of this compound in $CDCl_3$.

synthesis of this macrocycle and its incorporation in rotaxanes through its complexation of ureas and carbamates.

The ^{1}H NMR spectrum of an equimolar mixture of macrocycle **1** and 4-pyridone in $CDCl_3$ (Fig. 5b) shows significant changes in the chemical shifts of the resonances for the complex relative to those of the free species. The resonance arising from the macrocycle NH protons (H_c) is shifted downfield (+1.90 ppm) as a result of the hydrogen bonds between these protons and the carbonyl group of 4-pyridone. The upfield shifts of the resonances for the macrocycle phenylene protons (H_e and H_f, −0.31 and −0.35 ppm, respectively) and that of the 4-pyridone (−1.03 and −0.98 ppm) are characteristic of protons residing in the shielding zone of an aromatic ring. Additionally, the signals of the macrocycle methylene protons are shifted upfield (H_d and H_g, −0.05 and −0.29 ppm, respectively). These chemical shift changes suggest that the pyridone guest is located within the cavity of the macrocycle. From an ^{1}H NMR titration experiment, in which successive amounts of pyridone **2** were added to a solution of macrocycle **1**, we were able to estimate

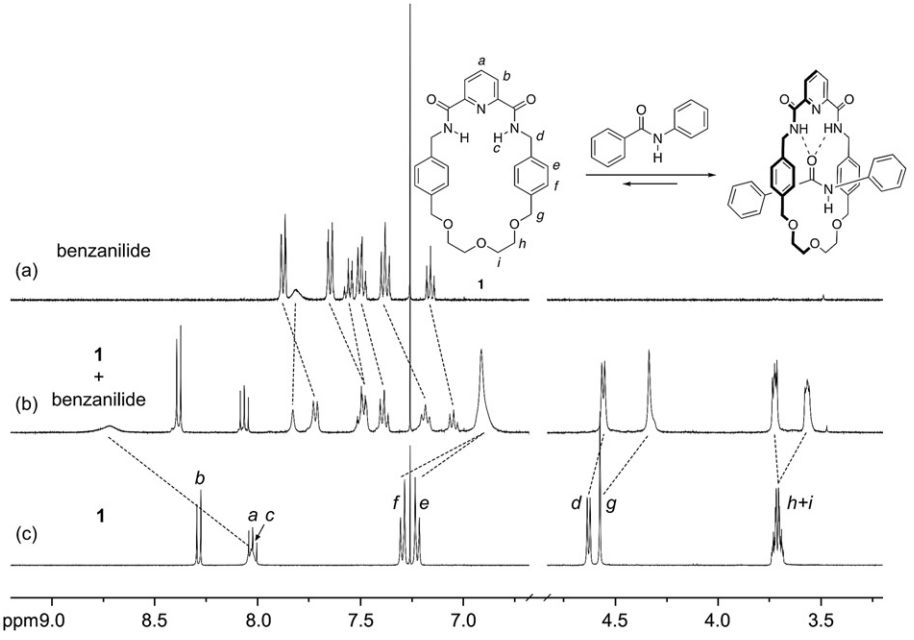

Figure 6. Partial ^{1}H NMR spectra (400.1 MHz, 25 °C, $CDCl_3$, 25 mM) of (a) benzanilide, (b) an equimolar mixture of macrocycle **1** and benzanilide and (c) macrocycle **1**. Dashed lines are shown to connect resonances for specific protons in the bound and unbound states.

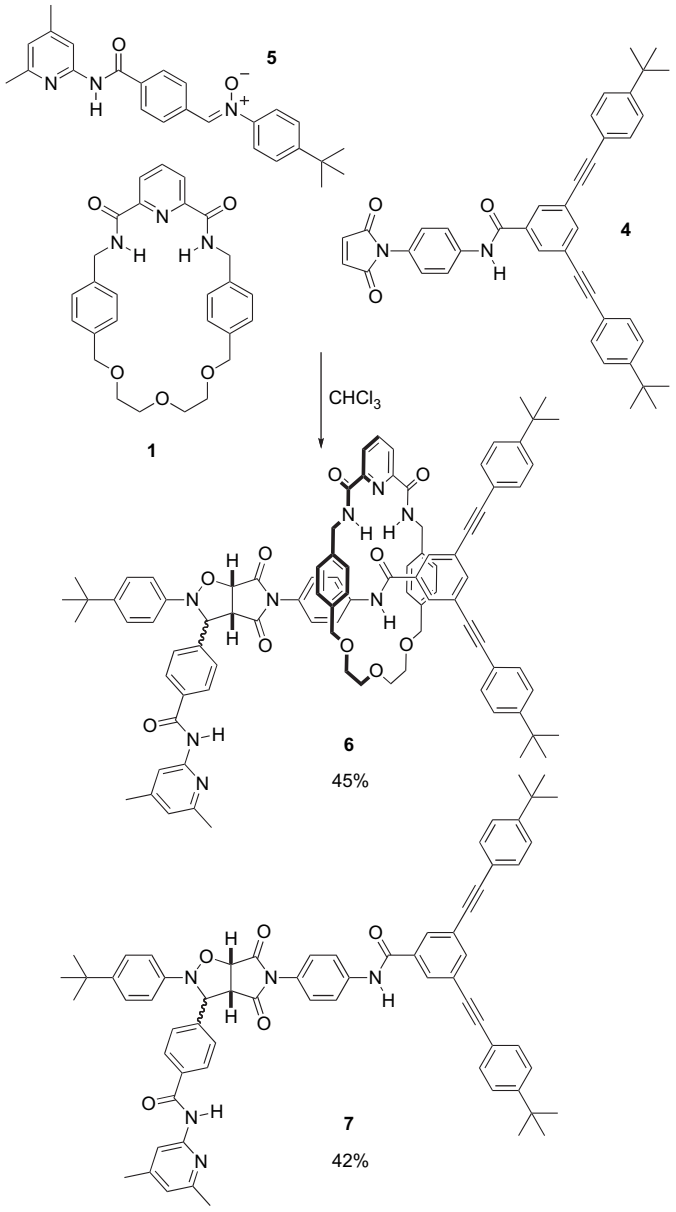

Figure 7. Design and synthesis of model rotaxane **6** and the corresponding thread **7** from macrocycle **1**, maleimide **4** and nitrone **5**. Both **6** and **7** are formed as mixtures of their *trans* and *cis* diastereoisomers.

the association constant for the [**1**·**2**] complex as 500±100 M^{-1} in $CDCl_3$ at 25 °C. Given the association between macrocycle **1** and 4-pyridone, we were able to exploit 4-pyridone as a template during the synthesis of macrocycle **1** itself: the yield of the cyclisation step increased from 29% to 39% using 1 equiv of 4-pyridone as a template (see Supplementary data).

We also prepared (see Supplementary data) an extended guest molecule **3** containing a 4-pyridone moiety and assessed its association with macrocycle **1**. The ^1H NMR spectrum of an equimolar mixture of macrocycle **1** and **3** in $CDCl_3$ (Fig. 5d) displays dramatic chemical shift changes, the origins of which are similar to those observed in the case of the complexation of 4-pyridone by **1**; the resonance arising from H_c is shifted downfield (+2.20 ppm) and both of H_e and H_f (−0.29 ppm) along with those of H_d and H_g (−0.04 and −0.32 ppm, respectively) are shifted upfield. In addition, the separation of the originally overlapping signals for the protons of H_h and H_i suggests hydrogen bonding between the pyridone NH and the ether oxygen atoms. These changes are consistent with the pseudorotaxane structure depicted in Figure 5, where the guest is threaded through the cavity of the host. From a series of ^1H NMR dilution experiments, involving a 1:1 mixture of macrocycle **1** and dialkynylpyridone **3**, we were able to estimate the association constant for the [**1**·**3**] complex as 1500±300 M^{-1} in $CDCl_3$ at 25 °C. It is worth noting at this point that the complex between **1** and **3** is in slow exchange on the chemical shift time scale at low concentrations, suggesting that some of the binding between **1** and **3** may be constrictive[19] in nature.

Although these results suggest that macrocycle **1** is a suitable host for pyridones and that the complex between the macrocycle and the extended guest **3** has the correct pseudorotaxane geometry, this recognition system has two fatal flaws. Firstly, the solubility of extended 2,6-substituted pyridone systems, such as **3**, is, at best, limited in the non-polar solvents necessary for efficient molecular recognition. Secondly, all of our synthetic efforts to incorporate this binding site into the linear component **L** of our replicating rotaxane design proved unsuccessful.

Therefore, the choice of binding site, which binds the macrocycle in building block **L**, had to be reassessed. Amides offered an attractive alternative binding site—their synthetic chemistry is much better developed than that of 2,6-substituted pyridone systems and they appeared to be adequate guests for macrocycle **1**. We established that diarylamides[20] are capable of associating with macrocycle **1** with a pseudorotaxane-type geometry by performing an additional binding experiment. The chemical shift changes observed in the ^1H NMR spectrum of an equimolar mixture of macrocycle **1** and benzanilide in $CDCl_3$ (Fig. 6b) are comparable to those observed for 4-pyridone and demonstrate that amides are suitable guests for macrocycle **1**. The strength of the complex formed between macrocycle **1** and benzanilide was estimated by measuring the association constant K_a by an ^1H NMR titration experiment and was found to be 160±20 M^{-1} in $CDCl_3$ at 25 °C. This value falls well short of our ideal value set out previously. However, given the synthetic tractability of amides when compared to 4-pyridones, we were prepared to accommodate their sub-optimal binding constants with macrocycle **1** in our revised designs.

In addition to the binding site, the design of our self-replicating rotaxane requires two further features: two reactive sites (bright red cartoons in Fig. 3) and an additional pair of complementary recognition sites (green cartoons in Fig. 3). We chose to use the 1,3-dipolar cycloaddition between a nitrone and a maleimide as the covalent bond forming reaction between the **L** and **S** components, and the association through two hydrogen bonds between an amidopyridine and a carboxylic acid as the complementary recognition sites. These choices were guided by our previous success[17] in exploiting these structural features in diastereoselective recognition-mediated reactions[21] and in the implementation of minimal[22] and reciprocal[23] self-replicating systems. In order to ensure that a simple rotaxane (i.e., one that is not capable of self-replication) can be formed using the cycloaddition reaction between a nitrone and a maleimide, amide-containing maleimide **4** (Fig. 7), which does not contain a recognition site on the stopper, macrocycle **1** and nitrone **5**, were synthesised (see Supplementary data). A mixture of maleimide **4** and macrocycle **1** was pre-equilibrated in $CDCl_3$ at −5 °C to allow the formation of a pseudorotaxane. The addition of nitrone **5** gave, after 3 days, rotaxane **6** in 45% yield, as a 2:1 mixture of its *trans* and *cis* diastereoisomers, and thread **7** in 42% yield, as a 5:1 mixture of its *trans* and *cis* diastereoisomers. In addition, 13% of unreacted maleimide **4** was recovered from the reaction mixture. The ^1H NMR spectrum of the *cis* diastereoisomer of rotaxane **6** (Fig. 8) reveals the features expected of a [2]rotaxane. Of particular note are the resonances arising from the macrocycle NH protons and the adjacent methylene groups (Fig. 8). In the free macrocycle, the resonance arising from the NH protons appears as

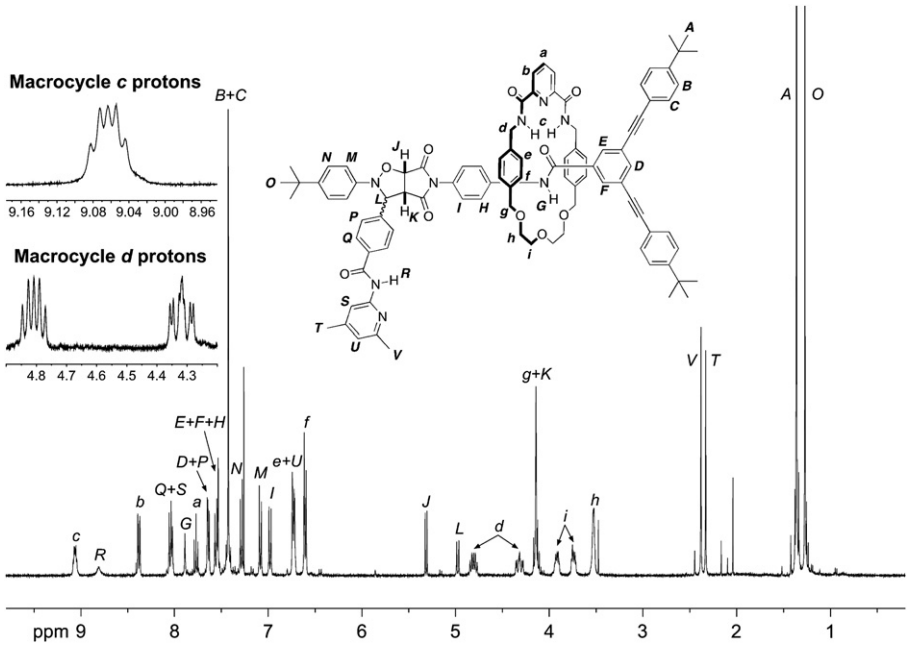

Figure 8. ^{1}H NMR spectrum (400.1 MHz, 25 °C, $CDCl_3$) of rotaxane *cis*-**6** together with proton assignments. Resonances arising from the macrocyclic component are labelled with small letters and those arising from the thread component are labelled with capital letters. The resonances arising from the c and d protons on the macrocycle are shown as inset partial spectra. Note that the sample also contains around 8% of *trans*-**6**. Resonances arising from *trans*-**6** are particularly evident in the pyridine CH_3 and aryl $C(CH_3)_3$ regions of the spectrum.

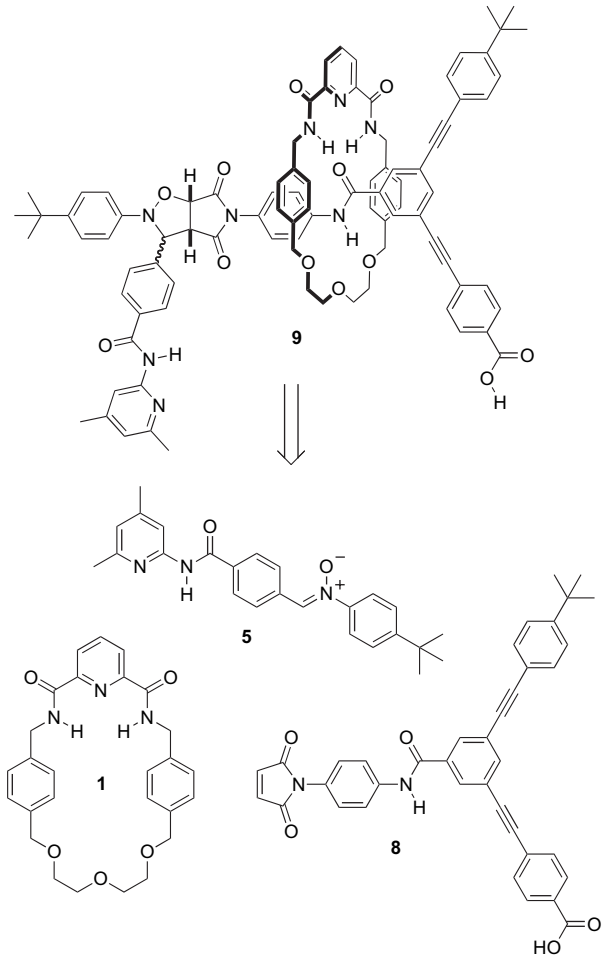

Figure 9. Retrosynthetic analysis of the design of replicating rotaxane **9** based on the model rotaxane **6**.

a triplet at δ 8.10 and that arising from the adjacent CH_2 as a doublet at δ 4.62. Upon rotaxane formation, the two methylene protons are rendered magnetically inequivalent as a result of the end-to-end asymmetry imposed by the thread. Further, the mirror plane present in the free macrocycle, which passes through the macrocycle perpendicular to the pyridine ring, is absent in the rotaxane. This loss is a result of the fact that the isoxazolidine ring formed in the cycloaddition reaction does not possess a matching element of symmetry. Therefore, the two NH protons and the four methylene protons are now all magnetically inequivalent and this leads to the observed complex signal patterns for the resonances arising from these protons (inset, Fig. 8). In addition, these resonances also show marked chemical shift changes as a result of the dramatic change in their local environments upon the interlocking of the thread and the macrocycle. The macrocycle amide NH proton resonances (c protons, Fig. 8) shift downfield from δ 8.10 to δ 9.06 and the macrocycle methylene proton resonances (d protons, Fig. 8) are now located at δ 4.81 and δ 4.32. There is also a strong upfield shift of the amide NH resonance of the macrocycle binding site (G proton, Fig. 8) in the rotaxane (δ 7.89) compared to the free thread (δ 8.55). This observation is once again consistent with the macrocycle being bound in the expected location in the rotaxane.

With these results in hand, we replaced one of the *tert*-butyl groups in maleimide **4** with a carboxylic acid recognition site affording the potential self-replicating rotaxane **9** (Fig. 9). In this design, the amidopyridine was incorporated into the stopper of compound **5** (building block **S**, Fig. 3), which also bears the nitrone reactive site. Compound **8** (building block **L**, Fig. 3) was designed by combining the maleimide, the amide-binding site and the carboxylic acid on the stopper. Both ends of nitrone **5**, the 4,6-dimethylpyridine ring and the *tert*-butyl phenyl ring are large enough to prevent the macrocycle forming[24] a pseudorotaxane with this component. Maleimide **8** was synthesised (see Supplementary data), but its extremely poor solubility in non-polar solvents forced us once again to reconsider the design of the system.

From our previous experience in designing recognition-mediated reactions, we envisaged that a solution to the solubility issues

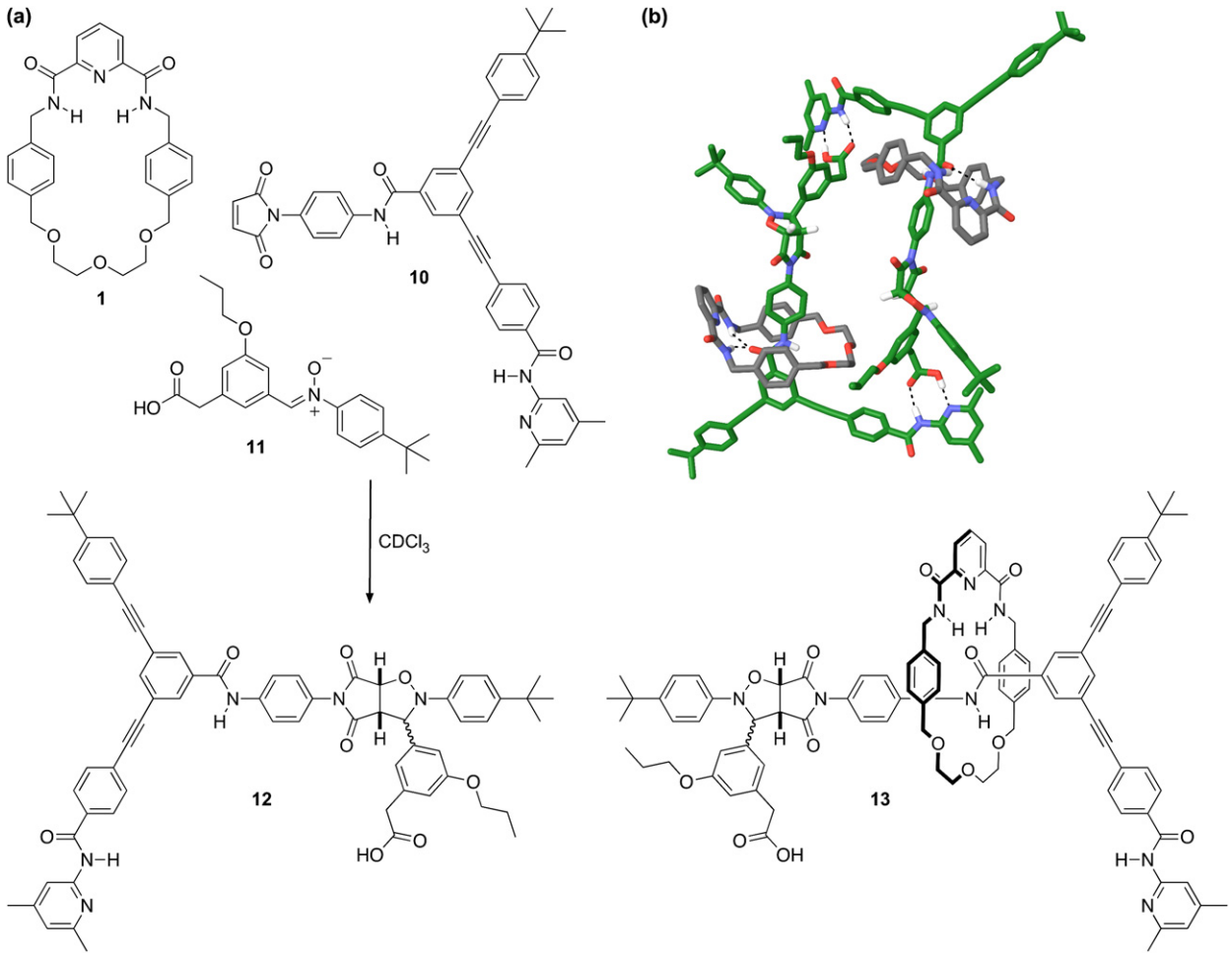

Figure 10. (a) Final design of a potential replicating rotaxane **13**. Nitrone **11** can react with maleimide **10** to afford the thread **12**. Alternatively, nitrone **11** can react with the pseudorotaxane complex [**1**·**10**] to afford the rotaxane **13**. The *trans* diastereoisomers of both thread **12** and rotaxane **13** are expected to be replicating. (b) Stick representation of the calculated structure (OPLS2005/GB/SA $CHCl_3$ solvation) of the product duplex of *trans*-**13**. Carbon atoms are coloured green in the linear components and grey in the macrocyclic components of the [2]rotaxanes, oxygen atoms are coloured red, nitrogen atoms are coloured blue and hydrogen atoms are coloured white. Most hydrogen atoms have been removed for clarity. Hydrogen bonds are shown as dashed lines.

was to reverse the location of the recognition sites on the **L** and **S** components of the rotaxane design. Accordingly, we designed a new system where the amidopyridine recognition site is situated on the stopper of malemide **10** (building block **L**) (Fig. 10a) and the carboxylic acid recognition site on the stopper of nitrone **11** (building block **S**) (Fig. 10a). Once again, the substitution pattern on nitrone **11** was designed to prevent pseudorotaxane formation between the nitrone and macrocycle **1**. Overall, these changes leave us with a design in which the *trans* diastereoisomer[25] of both the thread and the corresponding rotaxane is predicted computationally (Fig. 10b) to provide the correct geometry to support replication. Gratifyingly, all of the components of the potential replicator were sufficiently soluble in $CDCl_3$ to permit the study of their behaviour.

Reaction of nitrone **10** with maleimide **11** in $CDCl_3$ at 25 °C from starting concentrations of the two reagents of 20 mM afforded the thread **12** as a 7.9:1 *trans*/*cis* mixture of its diastereoisomers. After 8 h, the conversion was 49% (Fig. 11). When this reaction was repeated under the same conditions in the presence of 1 equiv (20 mM) of macrocycle **1**, the conversion after 8 h dropped (Fig. 11) to only 33%. More worryingly, the ratio of rotaxane **13** to thread **12** was 0.45:1, i.e., there was more thread present than rotaxane. The diastereoisomeric ratio of the thread in this reaction was now only 6:1 in favour of the *trans* stereoisomer. Interestingly, the ratio of diastereoisomers observed for rotaxane **13** was 1.4:1 in favour of the *cis* stereoisomer. We imagined that, given the sub-optimal binding constant[26] ($\sim$200 M^{-1}) for the association of macrocycle **1** with maleimide **10**, the poor performance of the system reflected the fact that insufficient pseudorotaxane [**1**·**10**] was present in solution. In order to address this problem, the reaction was repeated, again under the same conditions, but now in the presence of 3 equiv (60 mM) of macrocycle **1**—the conversion after 8 h (Fig. 11) dropped to only 26%. Gratifyingly, the ratio of rotaxane **13** to thread **12** was now 2.6:1, i.e., there was now more rotaxane present than thread. The diastereoisomeric ratio of the thread **12** in this reaction was still only 6:1 in favour of the *trans* stereoisomer and, in this case, the ratio of diastereoisomers observed for rotaxane **13** was 1.1:1 in favour of the *cis* stereoisomer. Although the addition of macrocycle operated in the manner expected—increasing the rotaxane/thread ratio—it also reduced the reactivity of the system markedly. Taken together, the results of the kinetic experiments were disappointing. The finally selected design targeted a *trans* selective replicator. Although the formation of the thread appears to be somewhat selective[27] for the *trans* diastereoisomer as expected, this selectivity is lost when macrocycle **1** is added to the reaction mixture. Indeed, the formation of rotaxane **13** is slightly selective for the *cis* diastereoisomer. Additionally, the overall conversion decreases rapidly when the macrocycle concentration is increased implying that the pseudorotaxane complex [**1**·**10**] and other, higher order, complexes incorporating [**1**·**10**], for some reason, are somewhat unreactive.

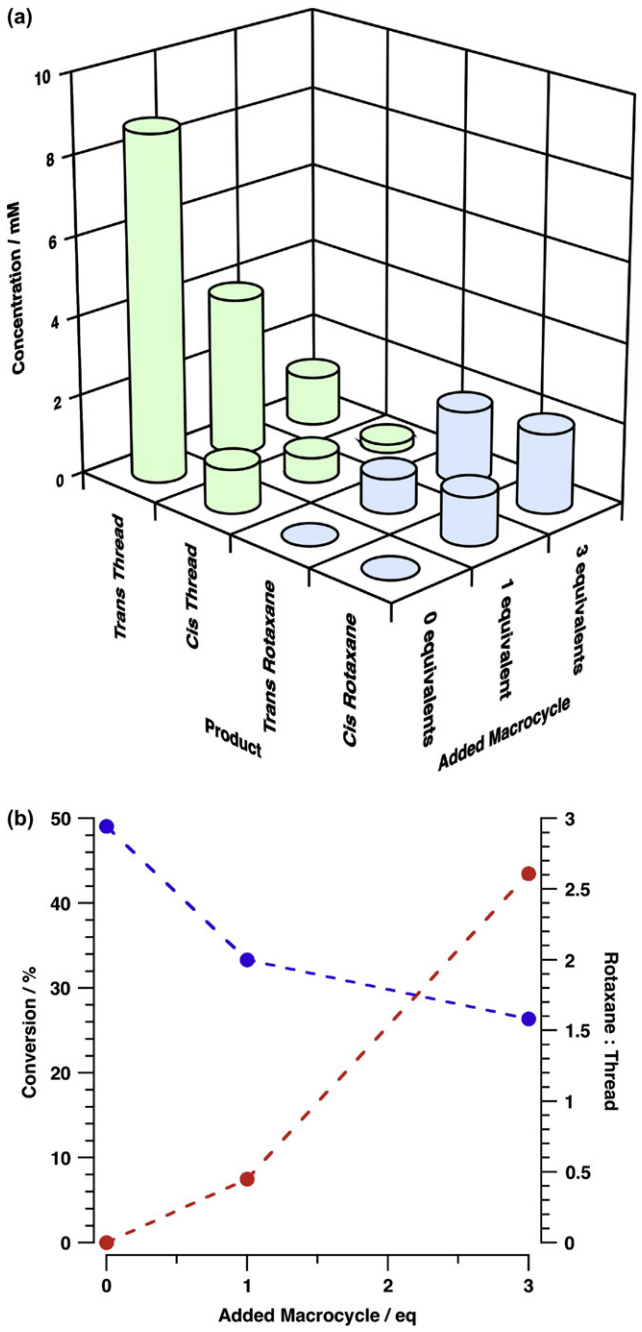

Figure 11. (a) Concentration of products (thread **12**=green columns, rotaxane **13**=blue columns) as a function of added macrocycle **1** for the kinetic experiments performed with macrocycle **1**. (b) Total conversion ([**12**]+[**13**] expressed as a percentage, blue points) and the ratio of rotaxane **13**/thread **12** (red points) as a function of the amount of added macrocycle **1**.

In order to understand the results of these kinetic experiments, we returned to the simplified kinetic model (Fig. 4) for rotaxane formation presented earlier. We used this model to predict (Fig. 12) the behaviour of the system with different loadings of macrocycle **1** present. We used a value for k_1, as before, of 1.67×10^{-3} M^{-1} s^{-1} and set the K_a for the pseudorotaxane complex as 200 M^{-1}. The rate constant for rotaxane formation was then fitted to obtain the best match with the selected metrics shown in Figure 12. Gratifyingly, we were able to reproduce the experimental data for the selected metrics using a value of $k_2=4.61\times10^{-4}$ M^{-1} s^{-1}.

The analysis presented above suggests that maleimide **10** becomes around four times less reactive within the [**1**·**10**] complex. We initially suspected that the low reactivity of the bound maleimide could originate from the mode of binding of the macrocycle. If the NH of the macrocycle formed hydrogen bonds with the carbonyl of the maleimide (Fig. 13a) instead of the carbonyl of the amide (Fig. 13b), the attack of the nitrone would be prevented through the steric obstruction of the π-face of the maleimide double bond. However, analysis of the complex formed between macrocycle **1** and model maleimide **14** using variable temperature ^{1}H NMR spectroscopy in $CDCl_3$, together with a ROESY experiment[28] performed at −30 °C, proved unambiguously that the macrocycle binds the amide-binding site only (see Supplementary data), and, therefore, the pseudorotaxane has the expected geometry shown in Figure 13b.

In order to investigate the reduced reactivity of the bound maleimide further, we turned to electronic structure calculations. Given the large size of the system, we were forced to use semi-empirical methods for these calculations. We wished to use a semi-empirical method that was capable of locating a high quality transition state structure for the dipolar cycloaddition. Hence, we located the transition state for the dipolar cycloaddition between *N*-phenylmaleimide and diphenylnitrone using density functional methods (B3LYP/6-31G+(d,p)). We then screened the available semi-empirical methods—AM1,[29] PM3,[30] RM1[31] and PM6[32]—against this transition state structure. The RM1 method gave the closest match to the DFT transition state structure and we therefore chose to proceed with the calculations involving the macrocycle using this method. We calculated the transition states accessed by the dipolar cycloaddition reaction between a model maleimide **15** and a model nitrone **16** using RM1 in the presence and in the absence of macrocycle **1**. The transition state structures located are shown in Figure 14. It is immediately apparent from the calculated structures that the association of macrocycle **1** with the amide-binding site exerts a remote steric effect[33] on the transition state. The *tert*-butyl group of the nitrone is located close to the bottom diethylene glycol loop of the macrocycle (Fig. 14, region X)—in fact, in region X (Fig. 14), part of the diethylene glycol loop and the *tert*-butyl group are essentially in van der Waals contact. This interaction is undoubtedly somewhat destabilising[34] to the transition state in the reaction between [**1**·**10**] and **11** when compared to the reaction between **10** and **11** in isolation. This observation also helps to explain the change observed in the diastereoselectivity of the cycloaddition between thread **12** (6:1 *trans*/*cis*) and rotaxane **13** (1:1.4 *trans*/*cis*). In rotaxane **13**, the *cis* diastereoisomer is slightly favoured, probably reflecting the fact that the *tert*-butyl group on nitrone **11** interacts more unfavourably with the macrocycle in the *trans* transition state compared with either the carboxymethylene or the propyloxy groups of **11** in the *cis* transition state.

3. Conclusions

We have presented a kinetic model for the integration of self-replication with the formation of a mechanically interlocked molecular architecture, namely a rotaxane. Ultimately, despite careful design, the system synthesised did not function as expected. This failure is a consequence of deficiencies in two important design criteria—one of which we recognised and the other was unanticipated. As a result of solubility and synthetic difficulty, we were forced to compromise with respect to the macrocycle binding site—substituting a pyridone ($K_a\sim1500$ M^{-1}) with an amide ($K_a\sim150$ M^{-1}). This compromise is clearly sub-optimal, since the association constant for the pseudorotaxane complex ([**L**·**M**], Fig. 3) must be as high as possible. This requirement is essential since the formation of this complex shuts down all kinetic pathways that involve free **L** and, hence, lead to the thread **T**. The depletion of free **L** therefore concentrates the kinetic flux in the autocatalytic cycle involving the rotaxane **R** (top right, Fig. 3). Secondly, the reactive site on **L** must be placed sufficiently far away from the binding site

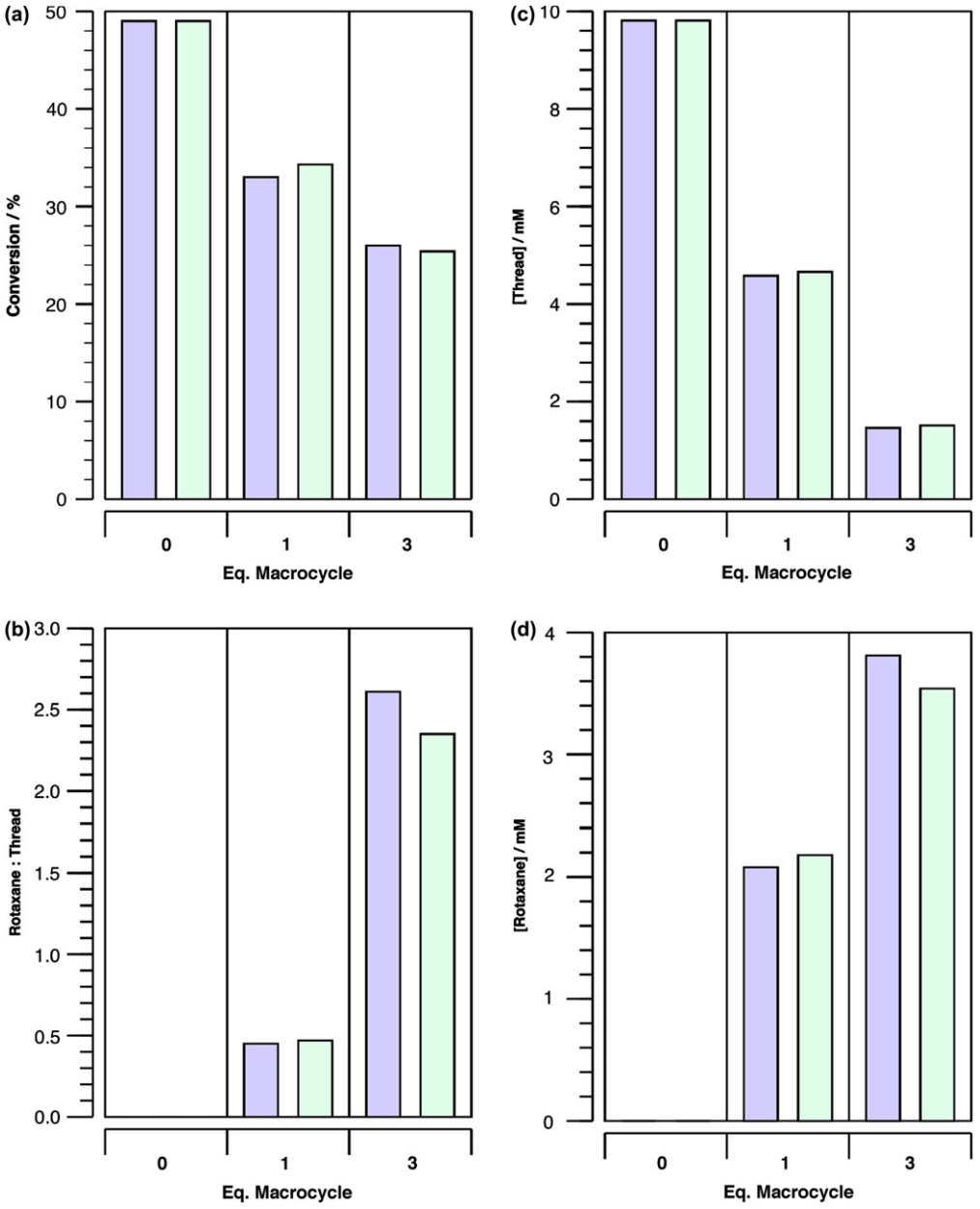

Figure 12. Comparison of experimental (blue) and calculated (green) metrics for the kinetic experiments performed using macrocycle **1**, maleimide **10** and nitrone **11**. The chosen metrics are (a) total conversion to cycloadduct expressed as a percentage, (b) ratio of rotaxane **13**/thread **12**, (c) concentration of thread **12** after 8 h and (d) concentration of rotaxane **13** after 8 h. Calculations used the kinetic scheme shown in Figure 4 with values of K_a=200 M^{-1} and k_1=1.67×10^{-3} M^{-1} s^{-1}. The best fit of all four metrics at the three concentrations of added macrocycle was obtained for k_2=4.61×10^{-4} M^{-1} s^{-1}.

to prevent the introduction of a supramolecular steric effect through the proximity of the macrocyclic component **M**. We are currently addressing these issues through improved designs using aggressive optimisation of the computational approaches described here. In addition, there are a number of other potential methods of integrating replication processes with mechanically interlocked molecular architectures and these are also currently under investigation in our laboratory.

4. Experimental

4.1. General procedures

Chemicals and solvents were purchased from standard commercial suppliers and were used as-received unless otherwise stated. Tetrahydrofuran (THF) was dried by heating to reflux in the presence of sodium/benzophenone under a N_2 atmosphere and was collected by distillation. Acetonitrile (CH_3CN) and dichloromethane (CH_2Cl_2) were dried by heating under reflux over calcium hydride and distilled under N_2.

Thin-layer chromatography (TLC) was performed on aluminium plates coated with Merck Kieselgel 60 F_{254}. Developed plates were air-dried and scrutinised under an UV lamp (366 nm), and where necessary, stained with ninhydrin or potassium permanganate to aid visualisation. Column chromatography was performed using Kieselgel 60 (0.040–0.063 mm mesh, Merck 9385) or MP Silica (silica gel, 0.032–0.063 mesh).

Melting points were determined using an Electrothermal 9200 melting point apparatus and are reported uncorrected. Microanalyses (C, H, N) were carried out at the University of St. Andrews.

^{1}H Nuclear Magnetic Resonance (NMR) spectra were recorded on a Bruker Avance II 400 (400.1 MHz), a Bruker Avance

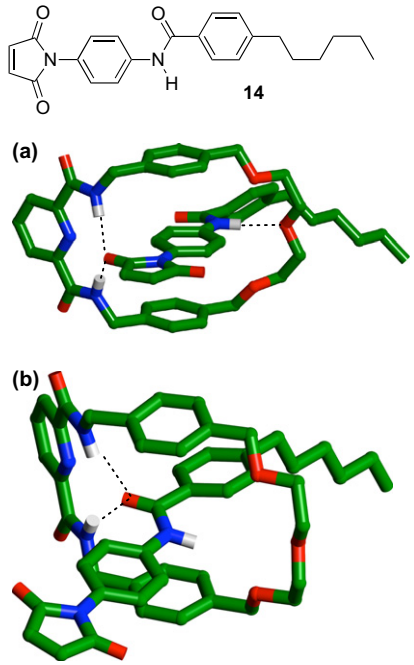

Figure 13. Stick representations of the calculated structures (OPLS2005/GB/SA $CHCl_3$ solvation) of the pseudorotaxane complexes formed between macrocycle **1** and maleimide **14**. (a) Macrocycle **1** amide NH groups hydrogen bond to a maleimide ring C=O oxygen and the maleimide amide NH hydrogen bonds to an ether oxygen atom on macrocycle **1**. (b) Macrocycle **1** amide NH groups hydrogen bond to maleimide amide C=O oxygen atom. In this geometry, the maleimide amide NH does not interact with the ether oxygens on macrocycle **1**. Carbon atoms are coloured green, oxygen atoms are coloured red, nitrogen atoms are coloured blue and hydrogen atoms are coloured white. Most hydrogen atoms have been removed for clarity. Hydrogen bonds are shown as dashed lines.

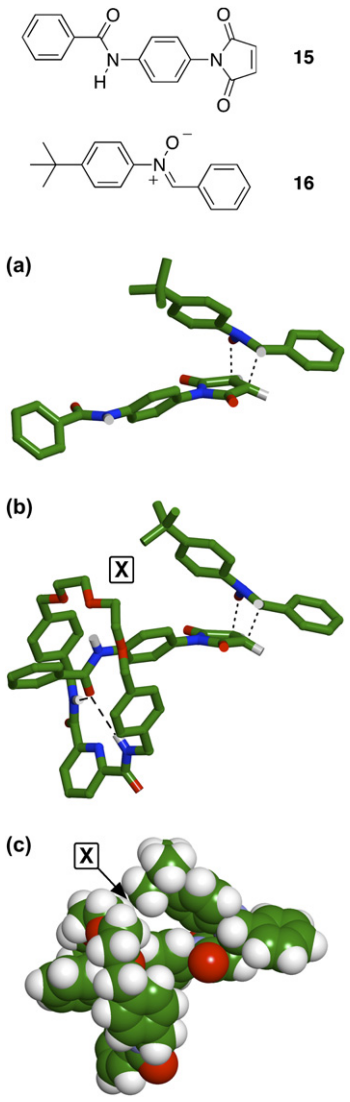

Figure 14. Stick representations of the calculated (RM1 semi-empirical method) transition state structures leading to the *trans* diastereoisomer for (a) the reaction between model maleimide **15** and model nitrone **16** and (b) the reaction between model nitrone **16** and the complex between model maleimide **15** and macrocycle **1**. In region X, the *tert*-butyl group of **16** is essentially in van der Waals contact with the diethylene glycol loop in macrocycle **1**, as illustrated in the space filling model (c). Carbon atoms are coloured green, oxygen atoms are coloured red, nitrogen atoms are coloured blue and hydrogen atoms are coloured white. Most hydrogen atoms have been removed for clarity. Hydrogen bonds are shown as dashed lines and forming bonds as dotted lines.

(300.1 MHz), a Bruker Avance (500.0 MHz) or a Varian UNITYplus 500 (500.1 MHz) spectrometer using deuterated solvent as the lock and the residual solvent as the internal reference in all cases. ^{13}C NMR spectra were recorded on a Bruker Avance 300 (75.5 MHz) or a Bruker Avance II 400 (100.6 MHz) spectrometer using the PENDANT or DEPTQ pulse sequences. All spectra were recorded at 298 K unless otherwise stated. All coupling constants (*J*) are quoted to the nearest 0.1 Hz. In the assignment of ^1H NMR spectra the symbols br, s, d, t, q and m denote broad, singlet, doublet, triplet, quartet and multiplet, respectively.

Electron impact mass spectrometry (EIMS) and high-resolution mass spectrometry (HRMS) were carried out on a Micromass GCT orthogonal acceleration time of flight mass spectrometer. Chemical Ionisation Mass Spectrometry (CIMS) was carried out on a Micromass GCT orthogonal acceleration time of flight mass spectrometer. Electrospray mass spectrometry (ESMS) and high-resolution mass spectrometry (HRMS) were carried out on a Micromass LCT orthogonal time of flight mass spectrometer.

4.2. General procedure for kinetic experiments

Masses of reagents were measured using a Sartorius BP 211D balance (±0.01 mg) and reagent solutions prepared by dissolving compounds in the appropriate volume of $CDCl_3$. Subsequent experimental samples, suitable for kinetic experiments, were prepared by using Hamilton gas-tight syringes to transfer solution to either a Wilmad 507PP or a 528PP NMR tube, which was then fitted with a polyethylene pressure cap to minimise solvent evaporation. Reaction mixtures were monitored systematically by 500 MHz ^1H NMR spectroscopy over 18 h. Concentrations were calibrated using an internal standard ($(Me_3Si)_4Si$) added to the reaction mixtures at a concentration of 600 μM. The extent of reaction for kinetic experiments was determined using the deconvolution of the appropriate product resonances using the tools available in Topspin (Version 2.0 pl 3, Bruker Biospin, Germany, 2006).

4.3. Computational methods

All molecular mechanics calculations were performed on a Linux workstation using the OPLS2005 forcefield together with the GB/SA solvation model for chloroform as implemented in Macromodel (Version 9.5, Schrödinger Inc., 2007). Electronic structure calculations were carried out using GAMESS-US[35] or MOPAC2007[36] running on a Linux cluster. The 64-bit Linux version dated 24 Mar 2007 (Revision 3) was used in all density functional calculations. The transition state for the reaction

between *N*-phenylmaleimide and diphenylnitrone was located by generation of an initial guess using the linear synchronous transit (LST) method and then refinement at the HF/6-31G(d) level of theory within GAMESS. This model transition state was then used to construct an initial guess for the transition state leading to the appropriate cycloadduct. This guess was refined at the B3LYP/6-31G+(d,p) level of theory to a transition state structure possessing single imaginary vibration that corresponded to the reaction coordinate. This transition state was then used for comparison purposes for those calculated using the semi-empirical methods AM1, PM3, RM1 and PM6. All semi-empirical electronic structure calculations were carried out using MOPAC2007. Version 8.032L was used in all calculations. In all cases, Eigen vector following was used to locate a transition state structure possessing single imaginary vibration that corresponded to the reaction coordinate.

4.4. Synthetic procedures

Preparative methods and characterisation data for compounds **1**, **3**, **4**, **5**, **8**, **10** and **11** and the intermediates leading to them are provided in Supplementary data.

*4.4.1. Rotaxane **6***

A mixture of macrocycle **1** (110 mg, 0.23 mmol), maleimide **4** (140 mg, 0.23 mmol) and chloroform (4.6 mL) was stirred at −5 °C for 1 h. Nitrone **5** (93 mg, 0.23 mmol) was then added to the reaction mixture at −5 °C. The reaction mixture was stirred at room temperature for 3 days. The solvent was evaporated under reduced pressure. The different products of the reaction were isolated by column chromatography (SiO_2, gradient from 9:1 to 3:7 cyclohexane/ethyl acetate) that afforded thread **7** (97 mg, 42%, *trans*/*cis* 5:1) as a pale brown solid and rotaxane **6** (153 mg, 45%, *trans*/*cis* 2:1) as a yellow solid. *Representative data for rotaxane (cis-**6**).* ^{1}H NMR (400.1 MHz, $CDCl_3$): δ=9.08–9.04 (dt, *J*=7.5, 3.8 Hz, 2H), 8.81 (br s, 1H), 8.40–8.37 (m, 2H), 8.05 (d, *J*=8.4 Hz, 2H), 8.02 (s, 1H), 7.89 (s, 1H), 7.77 (t, *J*=7.8 Hz, 1H), 7.65–7.63 (m, 1H+2H), 7.56 (d, *J*=8.9 Hz, 2H), 7.53 (d, *J*=1.4 Hz, 2H), 7.45–7.40 (m, 8H), 7.29 (d, *J*=8.8 Hz, 2H), 7.08 (d, *J*=8.8 Hz, 2H), 6.98 (d, *J*=9.0 Hz, 2H), 6.74–6.72 (m, 1H+4H), 6.61 (d, *J*=7.9 Hz, 4H), 5.31 (d, *J*=7.8 Hz, 1H), 4.98 (d, *J*=8.9 Hz, 1H), 4.81 (dt, *J*=15.0, 7.6 Hz, 2H), 4.36–4.28 (m, 2H), 4.17–4.13 (m, 1H+4H), 3.94–3.90 (m, 2H), 3.76–3.72 (m, 2H), 3.54–3.51 (m, 4H), 2.38 (s, 3H), 2.33 (s, 3H), 1.36 (s, 18H), 1.27 (s, 9H); ^{13}C NMR (100.6 MHz, $CDCl_3$): δ=173.73, 171.47, 164.95, 163.86, 163.29, 156.32, 152.18, 150.74, 149.24, 148.62, 144.04, 139.06, 138.96, 138.69, 137.22, 137.18, 136.59, 135.66, 134.81, 134.08, 131.52, 130.67, 128.83, 128.25, 128.11, 127.96, 126.30, 125.91, 125.70, 125.57, 125.43, 123.17, 120.83, 120.08, 119.79, 119.54, 111.88, 90.54, 87.38, 76.82, 73.53, 71.13, 70.82, 68.89, 54.76, 43.53, 35.00, 34.50, 31.39, 31.32, 23.74, 21.47; MS (ES): *m*/*z* (%)=1482 (100) $[M]^+$, 1483 (95) $[M+H]^+$; HRMS (MALDI): *m*/*z* calcd for $[M+H]^+$ $C_{93}H_{93}N_8O_{10}$ 1481.7015, found 1481.7056. *Representative data for thread (trans-**7**).* ^{1}H NMR (400.1 MHz, $CDCl_3$): δ=8.59 (s, 1H), 8.55 (s, 1H), 8.02 (s, 1H), 7.91–7.89 (m, 2H+2H), 7.76 (t, *J*=1.5 Hz, 1H), 7.64 (d, *J*=8.4 Hz, 2H), 7.60 (d, *J*=8.9 Hz, 2H), 7.43 (d, *J*=8.6 Hz, 4H), 7.37 (d, *J*=8.6 Hz, 4H), 7.25 (d, *J*=8.9 Hz, 2H), 7.08 (d, *J*=8.9 Hz, 2H), 6.76 (s, 1H), 6.45 (d, *J*=8.9 Hz, 2H), 5.82 (s, 1H), 5.04 (d, *J*=7.5 Hz, 1H), 3.97 (d, *J*=7.9 Hz, 1H), 2.41 (s, 3H), 2.33 (s, 3H), 1.32 (s, 18H), 1.27 (s, 9H); ^{13}C NMR (100.6 MHz, $CDCl_3$): δ=174.25, 172.84, 165.14, 164.66, 156.50, 152.27, 150.72, 150.44, 146.39, 146.20, 143.03, 138.74, 137.22, 135.33, 134.11, 131.58, 129.68, 127.92, 127.07, 126.99, 126.77, 126.47, 125.58, 124.64, 120.91, 120.61, 119.54, 114.12, 111.82, 91.54, 87.16, 77.48, 69.22, 57.33, 34.96, 34.31, 31.54, 31.25, 23.87, 21.43; MS (ES): *m*/*z* (%)=402 (100), 1007 (30) $[M+H]^+$; HRMS (ES): *m*/*z* calcd for $[M+H]^+$ $C_{66}H_{64}N_5O_5$ 1006.4907, found 1006.4901.

Acknowledgements

The financial support provided by the University of St. Andrews and EaStCHEM (graduate studentship to A.V.) is gratefully acknowledged. We thank Tomas Lebl and Melanja Smith for their assistance with NMR and Caroline Horsburgh for mass spectrometry.

Supplementary data

Supplementary data associated with this article can be found in the online version, at doi:10.1016/j.tet.2008.05.049.

References and notes

1. Ruben, M.; Rojo, J.; Romero-Salguero, F. J.; Uppadine, L. H.; Lehn, J.-M. *Angew. Chem., Int. Ed.* **2004**, *43*, 3644–3662.
2. Lukin, O.; Vögtle, F. *Angew. Chem., Int. Ed.* **2005**, *44*, 1456–1477.
3. (a) Sauvage, J.-P. *Acc. Chem. Res.* **1998**, *31*, 611–619; (b) Balzani, V.; Credi, A.; Raymo, F. M.; Stoddart, J. F. *Angew. Chem., Int. Ed.* **2000**, *39*, 3348–3391; (c) Schalley, C. A.; Beizai, K.; Vögtle, F. *Acc. Chem. Res.* **2001**, *34*, 465–476; (d) Feringa, B. L. *Molecular Switches*; Wiley-VCH: Weinheim, 2001; (e) Dietrich-Buchecker, C.; Jimenez-Molero, M. C.; Sartor, V.; Sauvage, J.-P. *Pure Appl. Chem.* **2003**, *75*, 1383–1393; (f) Flood, A. H.; Ramirez, R. J. A.; Deng, W.-Q.; Muller, R. P.; Goddard, W. A., III; Stoddart, J. F. *Aust. J. Chem.* **2004**, *57*, 301–322; (g) Tian, H.; Wang, Q.-C. *Chem. Soc. Rev.* **2006**, *35*, 361–374; (h) Balzani, V.; Credi, A.; Silvi, S.; Venturi, M. *Chem. Soc. Rev.* **2006**, *35*, 1135–1149; (i) Credi, A. *J. Phys.: Condens. Matter* **2006**, *18*, S1779–S1795; (j) Kay, E. R.; Leigh, D. A.; Zerbetto, F. *Angew. Chem., Int. Ed.* **2007**, *46*, 72–191; (k) Green, J. E.; Choi, J. W.; Boukai, A.; Bunimovich, Y.; Johnston-Halperin, E.; Delonno, E.; Luo, Y.; Sheriff, B. A.; Xu, K.; Shin, Y. S.; Tseng, H.-R.; Stoddart, J. F.; Heath, J. R. *Nature* **2007**, *445*, 414–417.
4. Chworos, A.; Severcan, I.; Koyfman, A. Y.; Weinkam, P.; Oroudjev, E.; Hansma, H. G.; Jaeger, L. *Science* **2004**, *306*, 2068–2072.
5. (a) Carbone, A.; Seeman, N. C. *Proc. Natl. Acad. Sci. U.S.A.* **2002**, *99*, 12577–12582; (b) Seeman, N. C.; Belcher, A. M. *Proc. Natl. Acad. Sci. U.S.A.* **2002**, *99*, 6451–6455; (c) Seeman, N. C. *Nature* **2003**, *421*, 427–431; (d) Seeman, N. C. *Chem. Biol.* **2003**, *10*, 1151–1159; (e) Liao, S.; Seeman, N. C. *Science* **2004**, *306*, 2072–2074; (f) Yan, H. *Science* **2004**, *306*, 2048–2049; (g) Samori, B.; Zuccheri, G. *Angew. Chem., Int. Ed.* **2005**, *44*, 1166–1181; (h) Gothelf, K. V.; Brown, R. S. *Chem.—Eur. J.* **2005**, *11*, 1062–1069.
6. (a) Lloyd Carroll, R.; Gorman, C. B. *Angew. Chem., Int. Ed.* **2002**, *41*, 4378–4400; (b) Becerril, H. A.; Stoltenberg, R. M.; Wheeler, D. R.; Davis, R. C.; Harb, J. N.; Wooley, A. T. *J. Am. Chem. Soc.* **2005**, *127*, 2828–2829; (c) Niemeyer, C. M. *Science* **2002**, *297*, 62–63.
7. Drexler, K. E. *Engines of Creation: The Coming Era of Nanotechnology*; Anchor: Doubleday, NY, 1986.
8. (a) Smalley, R. E. *Sci. Am.* **2001**, *285*, 76–77; (b) Whitesides, G. M. *Sci. Am.* **2001**, *285*, 78–83.
9. For reviews, see: (a) Orgel, L. E. *Nature* **1992**, *358*, 203–209; (b) Famulok, M.; Nowick, J. S.; Rebek, J., Jr. *Acta Chem. Scand.* **1992**, *46*, 315–324; (c) Wintner, E. A.; Conn, M. M.; Rebek, J., Jr. *Acc. Chem. Res.* **1994**, *27*, 198–203; (d) Wintner, E. A.; Rebek, J., Jr. *Acta Chem. Scand.* **1996**, *50*, 469–485; (e) Bag, B. G.; von Kiedrowski, G. *Pure Appl. Chem.* **1996**, *68*, 2145–2152; (f) Lee, D. H.; Severin, K.; Ghadiri, M. R. *Curr. Opin. Chem. Biol.* **1997**, *1*, 491–496; (g) Robertson, A.; Sinclair, A. J.; Philp, D. *Chem. Soc. Rev.* **2000**, *29*, 141–152; (h) Li, X.; Chmielewski, J. *Org. Biomol. Chem.* **2003**, *1*, 901–904; (i) Paul, N.; Joyce, G. F. *Curr. Opin. Chem. Biol.* **2004**, *8*, 634–639; (j) Patzke, V.; von Kiedrowski, G. *Arkivoc* **2007**, 293–310.
10. Some recent examples include: (a) Kindermann, M.; Stahl, I.; Reimold, M.; Pankau, W. M.; von Kiedrowski, G. *Angew. Chem., Int. Ed.* **2005**, *44*, 6750–6755; (b) Isaac, R.; Chmielewski, J. *J. Am. Chem. Soc.* **2002**, *124*, 6808–6809; (c) Li, X.; Chmielewski, J. *J. Am. Chem. Soc.* **2003**, *125*, 11820–11821; (d) Matsumura, S.; Takahashi, T.; Ueno, A.; Mihara, H. *Chem.—Eur. J.* **2003**, *9*, 4829–4837; (e) Lee, D. H.; Granja, J. R.; Martinez, J. A.; Severin, K.; Ghadiri, M. R. *Nature* **1996**, *382*, 525–528.
11. For comprehensive kinetic analyses of minimal systems, see: (a) von Kiedrowski, G. *Bioorganic Chemistry Frontiers*; Springer: Berlin, Heidelberg, 1993; Vol. 3, 113–146; (b) Reinhoudt, D. N.; Rudkevich, D. M.; de Jong, F. *J. Am. Chem. Soc.* **1996**, *118*, 6880–6889.
12. (a) Cram, D. J. *Angew. Chem., Int. Ed. Engl.* **1988**, *27*, 1009–1020; (b) Constable, E. C. *Comprehensive Supramolecular Chemistry*; Atwood, J. L., Davis, J. E. D., Macnicol, D. D., Vögtle, F., Eds.; Elsevier: New York, NY, 1996; p 218; (c) Rowan, S. J.; Hamilton, D. G.; Brady, P. A.; Sanders, J. K. M. *J. Am. Chem. Soc.* **1997**, *119*, 2578–2579; (d) Rowan, S. J.; Sanders, J. K. M. *J. Org. Chem.* **1998**, *63*, 1536–1546.
13. See also: Soai, K.; Shibata, T.; Sato, I. *Acc. Chem. Res.* **2000**, *33*, 382–390 and references cited therein Blackmond, D. G. *Asymm. Synth.* **2007**, 181–185.
14. (a) Allen, V. C.; Philp, D.; Spencer, N. *Org. Lett.* **2001**, *3*, 777–780; (b) Quayle, J. M.; Slawin, A. M. Z.; Philp, D. *Tetrahedron Lett.* **2002**, *43*, 7229–7233.
15. For reviews, see: (a) Dietrich-Buchecker, C. O.; Sauvage, J.-P. *Chem. Rev.* **1987**, *87*, 795–810; (b) Sauvage, J.-P. *Acc. Chem. Res.* **1990**, *23*, 319–327; (c) Amabilino,

D. B.; Stoddart, J. F. *Chem. Rev.* **1995**, *95*, 2725–2828; (d) Vögtle, F.; Dünnwald, T.; Schmidt, T. *Acc. Chem. Res.* **1996**, *29*, 451–460; (e) Breault, G. A.; Hunter, C. A.; Mayers, P. C. *Tetrahedron* **1999**, *55*, 5265–5293; (f) Fujita, M. *Acc. Chem. Res.* **1999**, *32*, 53–61; (g) Hubin, T. J.; Busch, D. H. *Coord. Chem. Rev.* **2000**, *200–202*, 5–52; (h) Schalley, C. A.; Weilandt, T.; Brüggemann, J.; Vögtle, F. *Top. Curr. Chem.* **2004**, *248*, 141–200; (i) Aricó, F.; Badjic, J. D.; Cantrill, S. J.; Flood, A. H.; Leung, K. C.-F.; Liu, Y.; Stoddart, J. F. *Top. Curr. Chem.* **2005**, *249*, 203–259; (j) Vickers, M. S.; Beer, P. D. *Chem. Soc. Rev.* **2007**, *36*, 211–225; (k) Loeb, S. J. *Chem. Soc. Rev.* **2007**, *36*, 226–235; (l) Kay, E. R.; Leigh, D. A. *Pure Appl. Chem.* **2008**, *80*, 17–29.

16. Until the advent of synthetic strategies that exploited molecular recognition for the construction of mechanically interlocked architectures, the study of such systems was confined to more theoretical aspects of such assembly. See: Walba, D. M. *Tetrahedron* **1985**, *41*, 3161–3212.
17. Kassianidis, E.; Philp, D. *Angew. Chem., Int. Ed.* **2006**, *45*, 6334–6348.
18. (a) Huang, Y.-L.; Hung, W.-C.; Lai, C.-C.; Liu, Y.-H.; Peng, S.-M.; Chiu, S.-H. *Angew. Chem., Int. Ed.* **2007**, *46*, 6629–6633. The syntheses of similar macrocycles have been reported: (b) Furusho, Y.; Matsuyama, T.; Takata, T.; Moriuchi, T.; Hirao, T. *Tetrahedron Lett.* **2004**, *45*, 9593–9597; (c) Leigh, D. A.; Thomson, A. R. *Org. Lett.* **2006**, *8*, 5377–5379.
19. The [**1**·**3**] complex has a larger association constant than the [**1**·**2**] complex despite the fact that both **2** and **3** having the same binding site. The slow exchange on the chemical shift time scale exhibited by the [**1**·**3**] complex suggests that the on and off rates for this complex are significantly lower than those for the [**1**·**2**] complex. This change in the on and off rates probably arises from a steric barrier imposed by a close complementarity between the mean free path through the cavity of macrocycle **1** and the phenylethynyl substituents present in **3**, rather than a greatly altered intrinsic binding of the pyridone ring to the macrocycle. The small size of macrocycle **1** is evident in other situations in this work (cf. complex [**1**·**10**]). For a discussion of slippage and constrictive binding, see: Fyfe, M. C. T.; Raymo, F. M.; Stoddart, J. F. *Stimulating Concepts in Chemistry*; Vögtle, F., Stoddart, J. F., Shibasaki, M., Eds.; VCH: Weinheim, 2000; pp 211–220.
20. Several groups have exploited the use of amides for the construction of rotaxanes over the past 15 years. For some examples, see: (a) Alvarez-Perez, M.; Goldup, S. M.; Leigh, D. A.; Slawin, A. M. Z. *J. Am. Chem. Soc.* **2008**, *130*, 1836–1838; (b) Fioravanti, G.; Haraszkiewicz, N.; Kay, E. R.; Mendoza, S. M.; Bruno, C.; Marcaccio, M.; Wiering, P. G.; Paolucci, F.; Rudolf, P.; Brouwer, A. M.; Leigh, D. A. *J. Am. Chem. Soc.* **2008**, *130*, 2593–2601; (c) Serreli, V.; Lee, C.-F.; Kay, E. R.; Leigh, D. A. *Nature* **2007**, *445*, 523–527; (d) Berna, J.; Brouwer, A. M.; Fazio, S. M.; Haraszkiewicz, N.; Leigh, D. A.; Lennon, C. M. *Chem. Commun.* **2007**, 1910–1912; (e) Chatterjee, M. N.; Kay, E. R.; Leigh, D. A. *J. Am. Chem. Soc.* **2006**, *128*, 4058–4073; (f) See Ref. 18c. (g) Kishan, M. R.; Parham, A.; Schelhase, F.; Yoneva, A.; Silva, G.; Chen, X.; Okamoto, Y.; Vögtle, F. *Angew. Chem., Int. Ed.* **2006**, *45*, 7296–7299; (h) Aucagne, V.; Leigh, D. A.; Lock, J. S.; Thomson, A. R. *J. Am. Chem. Soc.* **2006**, *128*, 1784–1785; (i) Berna, J.; Leigh, D. A.; Lubomska, M.; Mendoza, S. M.; Perez, E. M.; Rudolf, P.; Teobaldi, G.; Zerbetto, F. *Nat. Mater.* **2005**, *4*, 704–710; (j) Leigh, D. A.; Venturini, A.; Wilson, A. J.; Wong, J. K. Y.; Zerbetto, F. *Chem.—Eur. J.* **2004**, *10*, 4960–4969; (k) Keaveney, C. M.; Leigh, D. A. *Angew. Chem., Int. Ed.* **2004**, *43*, 1222–1224; (l) Kidd, T. J.; Loontjens, T. J. A.; Leigh, D. A.; Wong, J. K. Y. *Angew. Chem., Int. Ed.* **2003**, *42*, 3379–3383; (m) Lukin, O.; Kubota, T.; Okamoto, Y.; Schelhase, F.; Yoneva, A.; Muller, W. M.; Muller, U.; Vögtle, F. *Angew. Chem., Int. Ed.* **2003**, *42*, 4542–4545; (n) Gatti, F. G.; Lent, S.; Wong, J. K. Y.; Bottari, G.; Altieri, A.; Morales, M. A. F.; Teat, S. J.; Frochot, C.; Leigh, D. A.; Brouwer, A. M.; Zerbetto, F. *Proc. Natl. Acad. Sci. U.S.A.* **2003**, *100*, 10–14; (o) Hannam, J. S.; Kidd, T. J.; Leigh, D. A.; Wilson, A. J. *Org. Lett.* **2003**, *5*, 1907–1910; (p) Watanabe, N.; Kihara, N.; Furusho, Y.; Takata, T.; Araki, Y.; Ito, O. *Angew. Chem., Int. Ed.* **2003**, *42*, 681–683; (q) Bottari, G.; Dehez, F.; Leigh, D. A.; Nash, P. J.; Perez, E. M.; Wong, J. K. Y.; Zerbetto, F. *Angew. Chem., Int. Ed.* **2003**, *42*, 5886–5889; (r) Da Ros, T.; Guldi, D. M.; Morales, A. F.; Leigh, D. A.; Prato, M.; Turco, R. *Org. Lett.* **2003**, *5*, 689–691; (s) Alteri, A.; Gatti, F. G.; Kay, E. R.; Leigh, D. A.; Martel, D.; Paolucci, F.; Slawin, A. M. Z.; Wong, J. K. Y. *J. Am. Chem. Soc.* **2003**, *125*, 8644–8654; (t) Clegg, W.; Gimenez-Saiz, C.; Gatti, F. G.; Leigh, D. A.; Nepogodiev, S. A.; Slawin, A. M. Z.; Teat, S. J.; Wong, J. K. Y. *J. Am. Chem. Soc.* **2001**, *123*, 5983–5989; (u) Watanabe, N.; Furusho, Y.; Kihara, N.; Takata, T.; Kinbara, K.; Saigo, K. *Bull. Chem. Soc. Jpn.* **2001**, *74*, 149–155; (v) Furusho, Y.; Shoji, J.; Watanabe, N.; Kihara, N.; Adachi, T.; Takata, T. *Bull. Chem. Soc. Jpn.* **2001**, *74*, 139–147; (w) Hunter, C. A.; Low, C. M. R.; Packer, M. J.; Spey, S. E.; Vinter, J. G.; Vysotsky, M. O.; Zonta, C. *Angew. Chem., Int. Ed.* **2001**, *40*, 2678–2682; (x) Reuter, C.; Mohry, A.; Sobanski, A.; Vögtle, F. *Chem.—Eur. J.* **2000**, *6*, 1674–1682; (y) Reuter, C.; Vögtle, F. *Org. Lett.* **2000**, *2*, 593–595; (z) Leigh, D. A.; Murphy, A.; Slawin, A. M. Z.; Teat, S. J. *J. Am. Chem. Soc.* **1999**, *121*, 4124–4129; (aa) Seel, C.; Parham, A. H.; Safarowsky, O.; Hübner, G. M.; Vögtle, F. *J. Org. Chem.* **1999**, *64*, 7236–7242; (bb) Heim, C.; Affeld, A.; Nieger, M.; Vögtle, F. *Helv. Chim. Acta* **1999**, *82*, 746–759; (cc) Schmidt, T.; Schmieder, R.; Müller, W. M.; Kiupel, B.; Vögtle, F. *Eur. J. Org. Chem.* **1998**, 2003–2007; (dd) Jäger, R.; Baumann, S.; Fischer, M.; Safarowsky, O.; Nieger, M.; Vögtle, F. *Liebigs Ann.* **1997**, 2269–2273; (ee) Händel, M.; Plevoets, M.; Gestermann, S.; Vögtle, F. *Angew. Chem., Int. Ed.* **1997**, *36*, 1199–1201; (ff) Leigh, D. A.; Murphy, A.; Smart, J. P.; Slawin, A. M. Z. *Angew. Chem., Int. Ed.* **1997**, *36*, 728–732; (gg) Lane, A. S.; Leigh, D. A.; Murphy, A. *J. Am. Chem. Soc.* **1997**, *119*, 11092–11093; (hh) Johnston, A. G.; Leigh, D. A.; Murphy, A.; Smart, J. P.; Deegan, M. D. *J. Am. Chem. Soc.* **1996**, *118*, 10662–10663; (ii) Vögtle, F.; Jäger, R.; Händel, M.; Ottens-Hildebrandt, S.; Schmidt, W. *Synthesis* **1996**, 353–356; (jj) Vögtle, F.; Ahuis, F.; Baumann, S.; Sessler, J. L. *Liebigs Ann.* **1996**, 921–926; (kk) Vögtle, F.; Händel, M.; Meier, S.; Ottens-Hildebrandt, S.; Ott, F.; Schmidt, T. *Liebigs Ann.* **1995**, 739–743.
21. (a) Philp, D.; Robertson, A. *Chem. Commun.* **1998**, 879–880; (b) Bennes, R.; Philp, D.; Spencer, N.; Kariuki, B. M.; Harris, K. D. M. *Org. Lett.* **1999**, *1*, 1087–1090; (c) Robertson, A.; Philp, D.; Spencer, N. *Tetrahedron* **1999**, *55*, 11365–11384; (d) Bennes, R.; Babiloni, M. S.; Hayes, W.; Philp, D. *Tetrahedron Lett.* **2001**, *42*, 2377–2380; (e) Kassianidis, E.; Pearson, R. J.; Philp, D. *Chem.—Eur. J.* **2006**, *12*, 8798–8812; (f) Bennes, R.; Philp, D. *Org. Lett.* **2006**, *8*, 3651–3654.
22. (a) Kassianidis, E.; Pearson, R. J.; Philp, D. *Org. Lett.* **2005**, *7*, 3833–3836; (b) Pearson, R. J.; Kassianidis, E.; Philp, D. *Tetrahedron Lett.* **2004**, *45*, 4777–4780; (c) Pearson, R. J.; Kassianidis, E.; Slawin, A. M. Z.; Philp, D. *Chem.—Eur. J.* **2006**, *12*, 6829–6840.
23. Kassianidis, E.; Philp, D. *Chem. Commun.* **2006**, 4072–4074.
24. During the course of this work, we also discovered that nitrones can bind macrocycle **1**. Therefore, we designed nitrone **5** in order to prevent pseudorotaxane formation between macrocycle **1** and the nitrone.
25. The stereochemical labels *trans* and *cis* refer to the relative stereochemistry in the cycloadduct of the proton derived from the nitrone with respect to the ring junction protons (derived from the maleimide). In the *trans* diastereoisomer, the proton derived from the nitrone is on the opposite face of the fused ring system as the ring junction protons derived from the maleimide. In the *cis* diastereoisomer, the proton derived from the nitrone is on the same face of the fused ring system as the ring junction protons derived from the maleimide.
26. The association constant for the [**1**·**10**] complex was estimated at 230 M^{-1} from the 400 MHz ^1H NMR spectrum recorded at room temperature in $CDCl_3$. Under these conditions, exchange between bound and unbound species is slow on the chemical shift time scale and, therefore, a crude estimate of the association constant can be obtained simply by integrating resonances arising from the two species.
27. The dipolar cycloaddition between a nitrone and an *N*-aryl maleimide is rather insensitive to electronic effects and usually gives a *trans*/*cis* ratio between 2.7:1 and 3.3:1.
28. The 500 MHz ^1H NMR spectrum in $CDCl_3$ of this pseudorotaxane shows broad resonances at 25 °C as a result of intermediate exchange on the chemical shift time scale. Therefore, the ROESY experiment was performed at −30 °C (slow exchange limit).
29. Dewar, M. J. S.; Zoebisch, E. G.; Healy, E. F.; Stewart, J. J. P. *J. Am. Chem. Soc.* **1985**, *107*, 3902–3909.
30. Stewart, J. J. P. *J. Comput. Chem.* **1989**, *10*, 209–220.
31. Rocha, G. B.; Freire, R. O.; Simas, A. M.; Stewart, J. J. P. *J. Comput. Chem.* **2006**, *27*, 1101–1111.
32. Stewart, J. J. P. *J. Mol. Model.* **2007**, *13*, 1173–1213.
33. Altered reactivity of functional groups incorporated within mechanically interlocked structures is a well-established phenomenon. For some examples, see: (a) Leigh, D. A.; Pérez, E. M. *Chem. Commun.* **2004**, 2262–2263; (b) Zehnder, D. W.; Smithrud, D. B. *Org. Lett.* **2001**, *3*, 2485–2487; Oku, T.; Furusho, Y.; Takata, T. *Org. Lett.* **2003**, *5*, 4923–4925; Craig, M. R.; Hutchings, M. G.; Claridge, T. D. W.; Anderson, H. L. *Angew. Chem., Int. Ed.* **2001**, *40*, 1071–1074; Parham, A. H.; Windisch, B.; Vögtle, F. *Eur. J. Org. Chem.* **1999**, 1233–1238; Leigh, D. A.; Murphy, A.; Smart, J. P.; Slawin, A. M. Z. *Angew. Chem., Int. Ed.* **1997**, *36*, 728–732; Asakawa, M.; Brown, C. L.; Menzer, S.; Raymo, F. M.; Stoddart, J. F.; Williams, D. J. *J. Am. Chem. Soc.* **1997**, *119*, 2614–2627.
34. Calculation of the energies of activation using thermochemical data derived from the RM1 calculations estimates that the activation barrier for the reaction of the [**1**·**15**] complex is around 6 kcal mol^{-1} higher than that for the reaction of **15** in the absence of macrocycle. Whilst the absolute value of this difference is unlikely to be correct at this low level of theory, it does support, at least qualitatively, the conclusion that binding of the macrocycle introduces a supramolecular steric effect into the system.
35. (a) Schmidt, M. W.; Baldridge, K. K.; Boatz, J. A.; Elbert, S. T.; Gordon, M. S.; Jensen, J. H.; Koseki, S.; Matsunaga, N.; Nguyen, K. A.; Su, S.; Windus, T. L.; Dupuis, M.; Montgomery, J. A. *J. Comput. Chem.* **1993**, *14*, 1347–1363; (b) Gordon, M. S.; Schmidt, M. W. *Theory and Applications of Computational Chemistry: The First Forty Years*; Dykstra, C. E., Frenking, G., Kim, K. S., Scuseria, G. E., Eds.; Elsevier: Amsterdam, 2005; p 1167.
36. Stewart, J. J. P. *MOPAC2007*; Stewart Computational Chemistry: Colorado Springs, CO, USA, 2007; http://openmopac.net.